



# FC PEM Model for Compressor Assignment and Overall Optimization

Program TRIO, ev. č. projektu.: **FV40072**

Název projektu: **SENCAT - Pokročilé materiály palivových článků pro udržitelnou energetiku**

WP 1.B Selection and Tests of Basic Elements, Compressor Specification and Control (Výběr a testování základních prvků, návrh kompresoru a automatizace)

WP 1.C Model of a Full-scale Stack of Fuel Cell (Sestavení modelu plnorozměrového svazku palivového článku )

Authors

Prof. Ing. Jan Macek, DrSc., vedoucí týmu C

3. ledna 2020

Ing. Pavel Brynych, PhD. - výzkumný pracovník (simulace v GT Suite)

Ing. Vít Doleček, PhD. - výzkumný pracovník (simulace v GT Suite)

Ing. Radek Tichánek, PhD. - výzkumný pracovník (požadavky na vzduchovou cestu)

Ing. Rastislav Toman - výzkumný pracovník (požadavky na vzduchovou cestu)

Ing. Jiří Vávra, Ph.D. - výzkumný pracovník (vodíková cesta a vlastnosti vodíku)

Centrum vozidel udržitelné mobility FS ČVUT v Praze, U 12 201

**Zpráva Z 19-20, Praha 2019**

## Obsah

Abstract .....	2
1. Introduction.....	3
2. Electrochemical Part of PEM FC .....	6
3. Gas Properties for PEM FC Model .....	10
4. Air Path Model.....	12
5. The First Results .....	17
6. Possibilities of Compressor and Turbocharger Procurement .....	19
7. Conclusion .....	19
8. Symbols and Acronyms .....	20
Subscripts .....	21
Acronyms.....	22
9. References.....	23

## Abstract

The report describes basic principles and features of a PEM FC air-path model, compressor characterization and specification, suitable for calibration by experiments and following optimization. The model describes all basic parts by their maps obtained from experiments, using regression models. It is written as large Excel programming language (Visual Basic) code. It is suitable to be run using standard optimization codes, e.g., ModeFrontier, using multi-variable genetic algorithm codes.

The basic modules are prepared for usage in a beta-version of the current version of GT Suite simulation device.

## 1. Introduction

The goal of a current project SENCAT is to do research and development of advanced nanocatalysts for the production of FC PEM stack-based electric generators with competitive prices. CTU in Prague contributes by the partial **goal 3** (part C of the project), which is **modelling and simulation of air-side chargers and compressors for these electric power generators**.

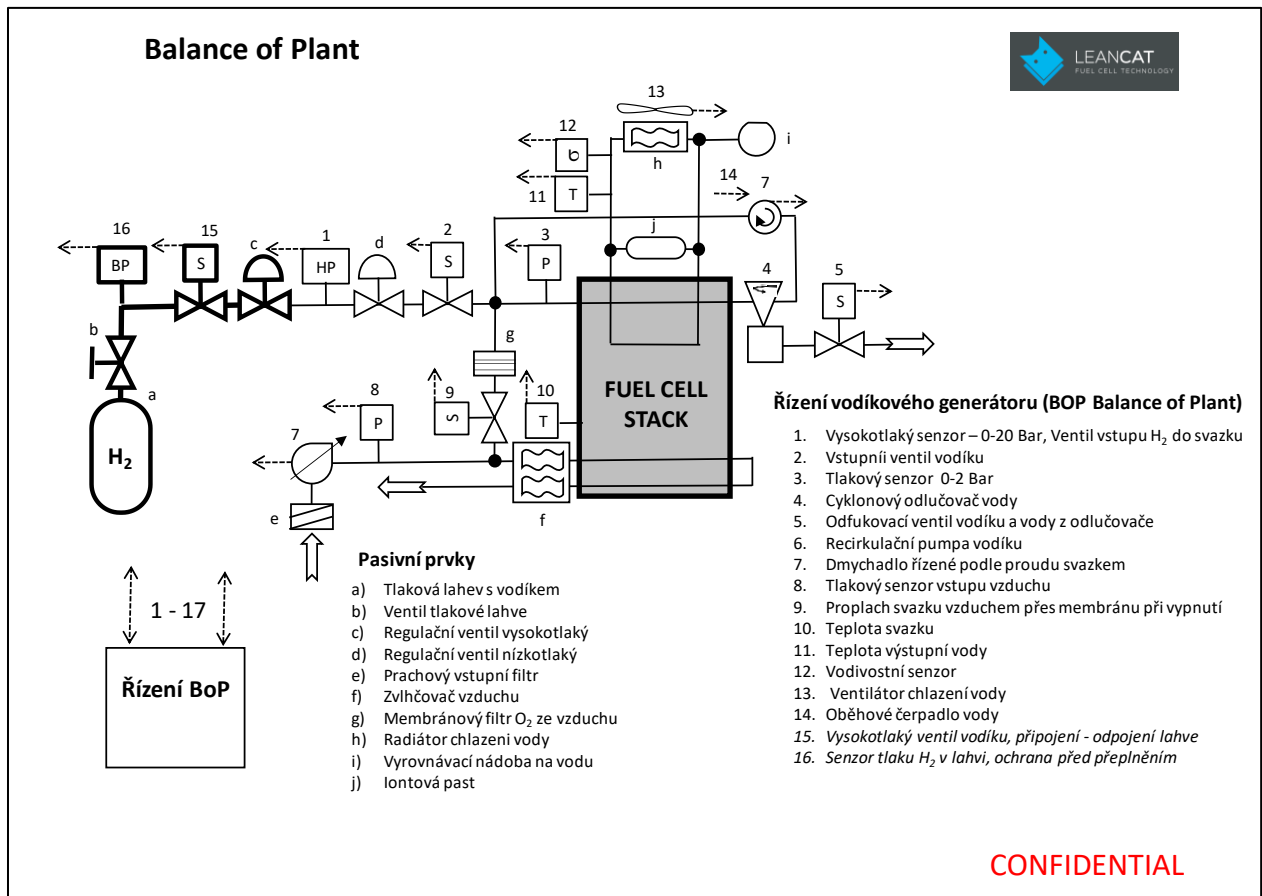


Figure 1 Basic lay-out of electrically supercharged PEM FC powerplant, report to SENCAT project application

PEM fuel cells are promising transformer of electric energy, stored in the form chemical energy of hydrogen, back to electric energy in stationary and vehicle facilities - Figure 1.

High efficiency of PEM FC have to be compromised with the volume and mass of energy facility, which is important for vehicle implementation especially. In such cases, supercharging at air side is used. Standard boost pressure achieves 2-3 bars (absolute pressure), which in connection with high air/fuel ratio means quite high internal power load, reducing net power at stack outlet. An expansion turbine, mostly in the form of a turbocharger, may help, reducing simultaneously temperature at atmospheric pressure side, which can be associated with a source of water for air humidification by either water injection downstream of the last air compressor and air cooler or by a contact humidifier at system inlet. Due to low temperature of exhaust gas (rest gases from air after consuming part of oxygen, water steam and aerosol of liquid water and traces of hydrogen), the turbine of realistic isentropic efficiency is not able to recover all compression work. Either e-turbo (Figure 19) or turbocharger and e-booster (Figure 2) have to be used as competitors to standard e-boosted design (Figure 1 or Figure 3). Other compressors or circuit circulation chargers, pumps and

vans for cooling circuit are driven electrically, as well. The basic system lay-out for modelling purposes is plotted as general scheme in Figure 2. Not all parts are used in every designed PEM FC but the model is prepared to take into account possible amendments of a lay-out.

All heat and mass (humidifying) exchangers and the stack itself cause significant pressure drops, featuring turbulent (kinetic energy) losses, dependent roughly on velocity squared, and laminar flow friction losses, proportional to velocity.

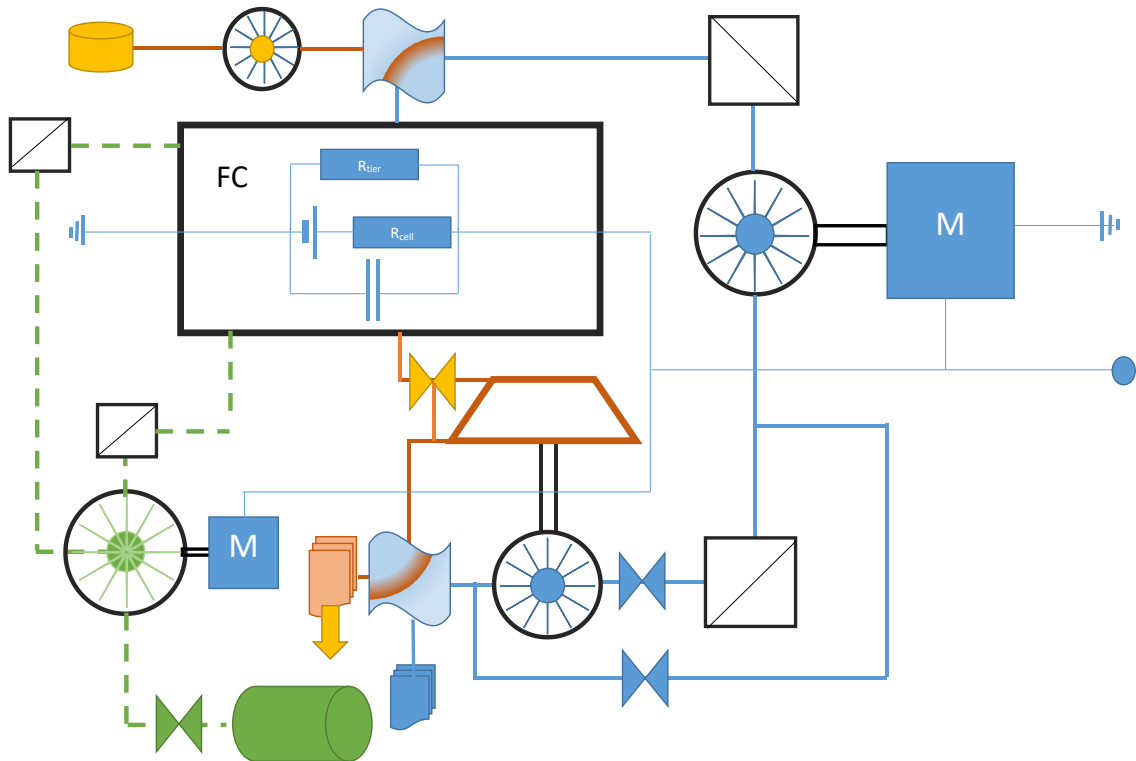


Figure 2 Lay-out of general PEM FC system model without a scheme of cooling circuit. The stack is modelled as a source of electromotive force, loaded by internal serial and parallel resistances.

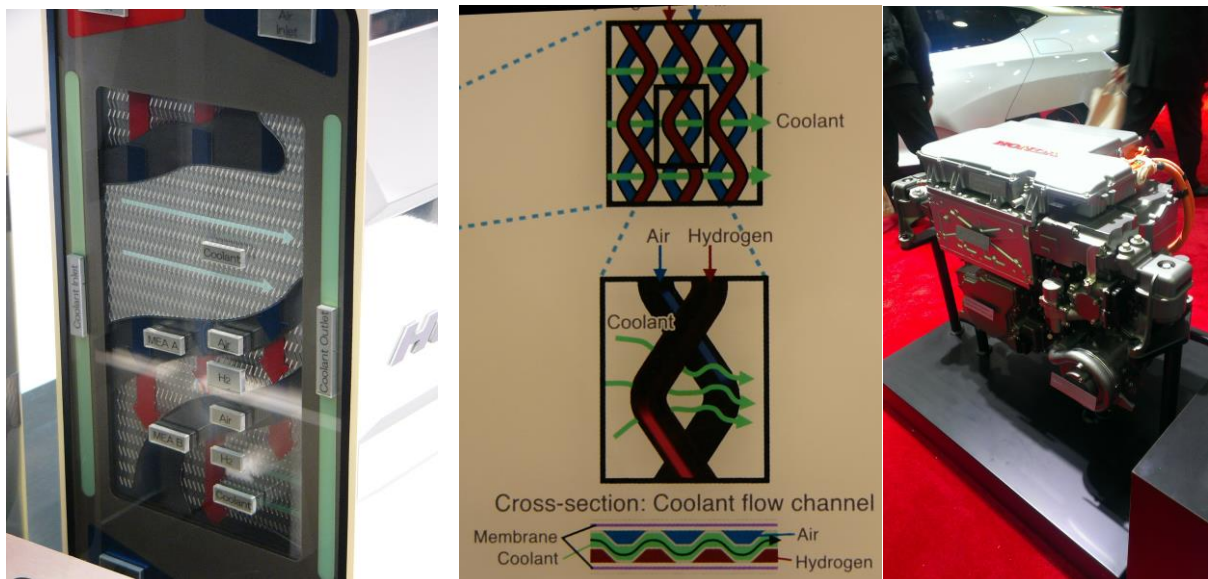
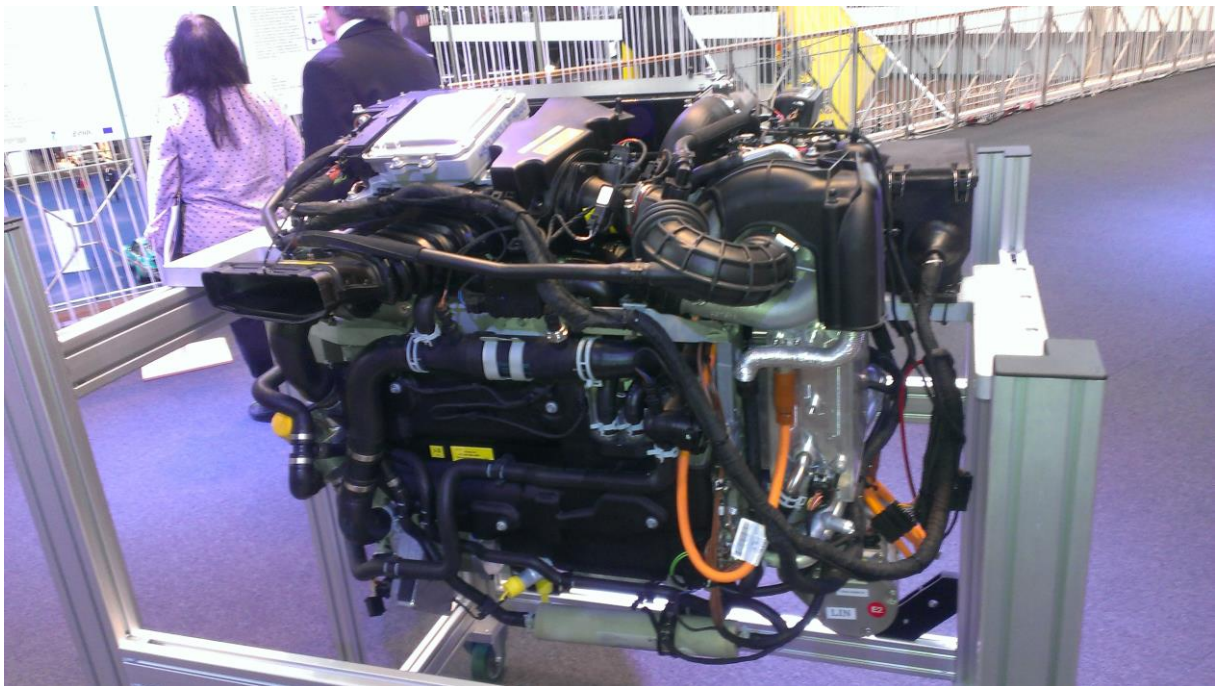


Figure 3 Honda cross-flow FC (principle Alfa Laval Plate Heat Exchangers), e-booster left below the stack– SAE Congress 2009, Jan Macek





*Figure 4 Compact lay-out of Mercedes Benz FC (Eucar Conference 2013, Jan Macek)*

The automotive PEM FC are designed in very compact way, as shown in Figure 4 and Figure 5, mentioned in presentation to [10]. The compact design limits cross-section areas of pipes and it causes and together with frequent bends of pipes significant pressure losses in connecting pipes and manifolds.



Figure 5 Toyota FC in a car (SAE Congress 2015, Jan Macek)

## 2. Electrochemical Part of PEM FC

The current model is not primarily focused on simulation of electrochemistry and internal specie-transfer processes of PEM FC, described very carefully, e.g., in [8] and influence of PE membrane humidification as described in [9]. However, basic traces of PEM FC efficiency dependence on loading power have to be simulated, since they influence significantly the state of air at inlet and in exhaust gas (rest of air gases, steam and water aerosol). The basic energy conservation (Stodola) yields

$$P_{net} = -K_{cool,P} P_{net} - \sum_i P_{eM,i} + \dot{m}_{air} h_{air,in} + \dot{m}_{fuel} h_{fuel,in} - (\dot{m}_{air} + \dot{m}_{fuel}) h_{v,out} \quad (1)$$

The fixed parameter for iterations is gross power of a tier. The other set input parameters for the whole procedure are

- air excess  $\lambda$  (inverted value of equivalence ratio), i.e., normalized “air” to fuel ratio, which takes into account composition of both gas at air and fuel sides, considering their humidity and traces of other gases, e.g., hydrogen at air side,
- relative cooling heat flux  $K_{cool,P}$
- boosted pressure at PEM FC inlet  $p_{FC,in}$ .

Then, the largest iteration loop is started by estimation of correction factor between net and gross power, gross efficiency being based on cell and tier losses (see below). Net power and gas flows at both sides of PEM FC are

$$\begin{aligned} P_{net} &= P_{gross} \eta_{net-gross} \\ \dot{m}_{fuel} &= \frac{P_{gross}}{H_u \eta_{gross}} \\ \dot{m}_{air} &= \dot{m}_{fuel} \lambda L_t \end{aligned} \quad (2)$$

The gross power is extracted from fuel chemical energy with efficiency, determined by empirically modified Tafel curve of a cell (reflected by Figure 6 in the left-hand side “theoretical” efficiency curve), followed by ohmic part.

Nonlinear regression representation of losses in the form prepared for any power device in [13] or [14], was applied for dependence on power output normalized by rated output and loss normalized by the current (!) power output

$$L_{rel, cell} = \frac{L_{cell}}{P_{cell=gross}} = [A_0 + A_1 P_{rel} + A_2 P_{rel}^x + A_3 P_{rel}^y + A_4 P_{rel}^z] \quad (3)$$

$$\eta_{cell} = \frac{P_{cell}}{P_{chem}} = \frac{P_{cell}}{P_{cell} + L_{rel, cell}} = \frac{1}{1 + L_{rel, cell}}$$

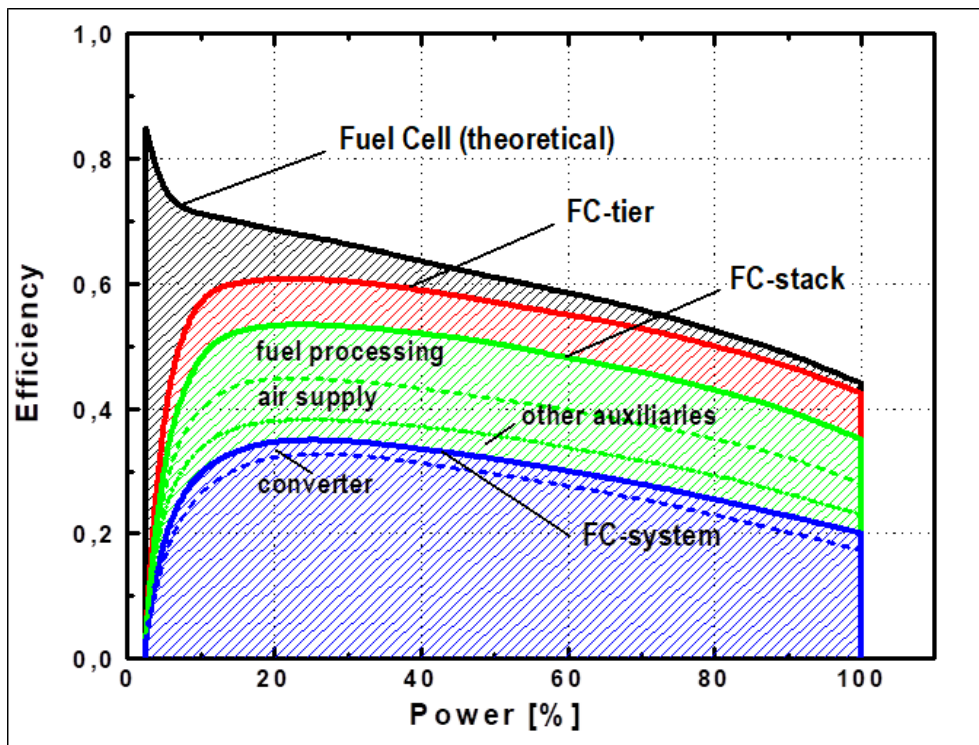


Figure 6 Example of loss distribution in a PEM FC cell, tier and stack - [1]

The following efficiencies can be calculated from additional losses, again normalized to the current outputs using efficiencies in iterative way (or solving directly the quadratic equations for relative losses)



$$\begin{aligned}
 \eta_{tier} &= \frac{1}{1 + \frac{L_{cell}}{P_{cell}} \frac{P_{cell}}{P_{tier}} + \frac{L_{tier}}{P_{tier}}} = \frac{1}{1 + L_{rel,cell} \frac{P_{tier} + L_{tier}}{P_{tier}} + L_{rel,tier}} = \frac{1}{1 + L_{rel,cell} (1 + L_{rel,tier}) + L_{rel,tier}} \\
 \eta_{stack} &= \frac{1}{1 + \frac{L_{cell}}{P_{cell}} \frac{P_{cell}}{P_{tier}} \frac{P_{tier}}{P_{stack}} + \frac{L_{tier}}{P_{tier}} \frac{P_{tier}}{P_{stack}} + \frac{L_{stack}}{P_{stack=net}}} = \\
 &= \frac{1}{1 + L_{rel,cell} (1 + L_{rel,tier}) (1 + L_{rel,stack}) + L_{rel,tier} (1 + L_{rel,stack}) + L_{rel,stack}}
 \end{aligned} \tag{4}$$

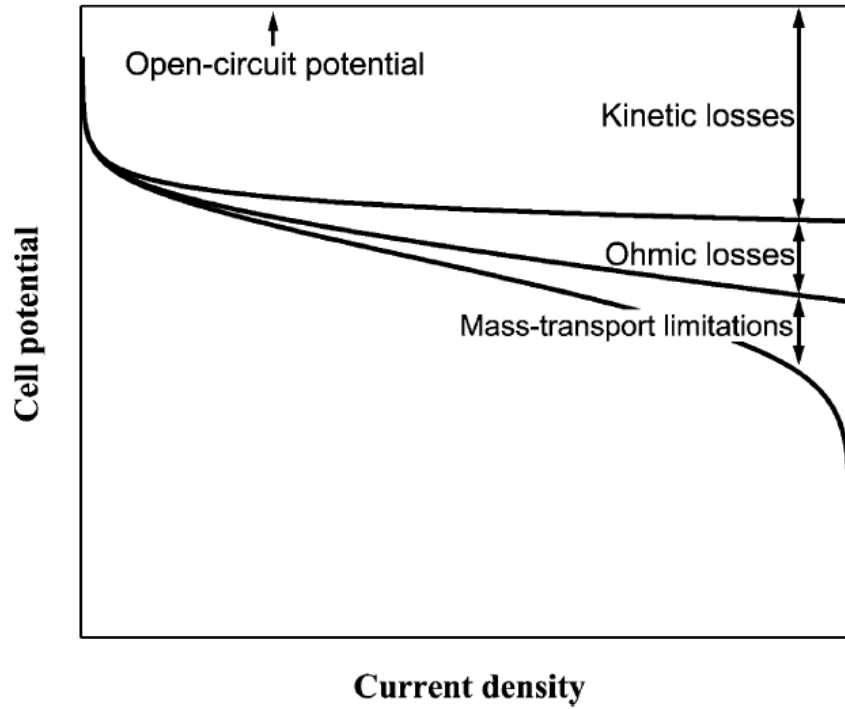


Figure 7 Explanation of basic losses inside fuels cell tier [8]

A very simple model according roughly to [8], is plotted inside FC element in Figure 2, using serial and parallel –“short circuiting” – resistances. It can explain tier losses at higher load (current). The relative loss at serial resistance yields from power loss a fictitious voltage can be found from

$$L_{rel,cell} = \frac{R_{cell} I^2}{P_{cell}} = \frac{R_{cell}}{P_{cell}} \left( \frac{P_{cell}}{U} \right)^2 = R_{cell} P_{cell} \left( \frac{1}{U} \right)^2 \Rightarrow U^2 = \frac{R_{cell} P_{cell}}{L_{rel,cell}} \tag{5}$$

Then, the tier loss caused by parallel resistance (influence of cooling water conductivity, short-circuiting bipolar plates), yields



$$L_{rel,tier} = \frac{R_{tier} I_{parallel}^2}{P_{tier}} = \frac{R_{tier} (1 + L_{rel,tier})}{P_{cell}} \left( \frac{U}{R_{tier}} \right)^2 = (1 + L_{rel,tier}) \frac{R_{cell} P_{cell}}{R_{tier}^2 P_{cell}} \frac{1}{L_{rel,cell}} \quad (6)$$

$$L_{rel,tier} \left( 1 - \frac{R_{cell}}{R_{tier}^2} \frac{1}{L_{rel,cell}} \right) = \frac{R_{cell}}{R_{tier}^2} \frac{1}{L_{rel,cell}} \Rightarrow L_{rel,tier} = \frac{K \frac{1}{L_{rel,cell}}}{1 - K \frac{1}{L_{rel,cell}}}$$

Even this simple approach yields quite satisfactory results for loads higher than 15% (outside of Tafel region), as presented in Figure 8

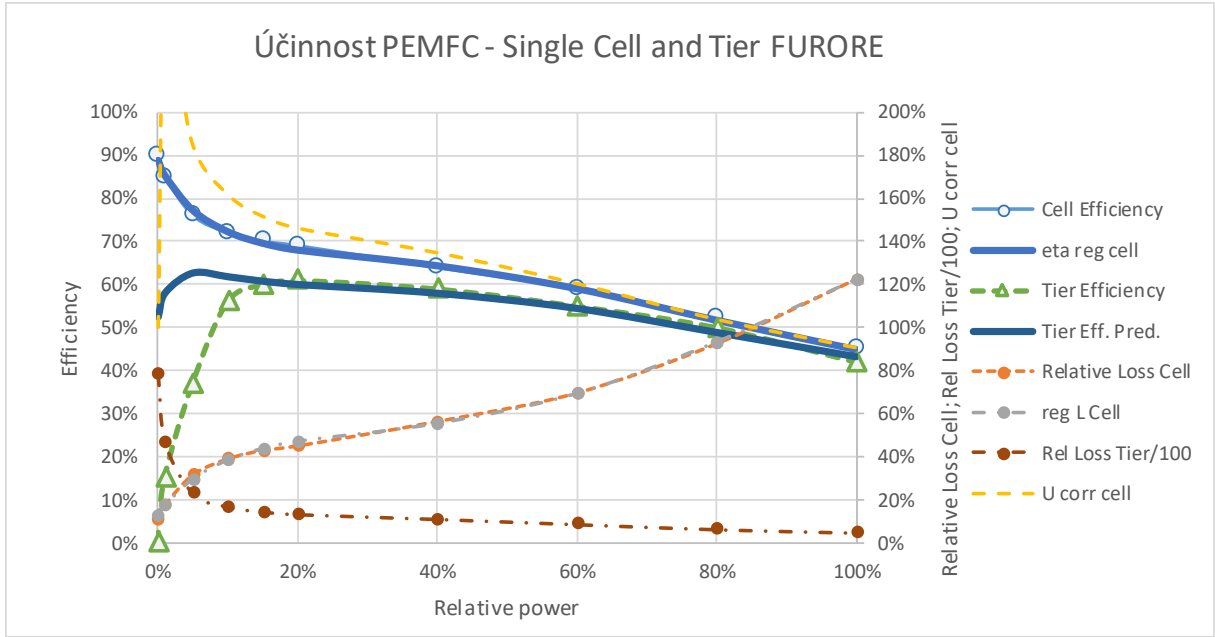


Figure 8 Model of cell efficiency from [1] based on model in [11] and correction to tier features assuming constant ohmic resistances in Figure 2 and Figure 6

The detailed models of cell and tier are not necessary for the current project goals, although they deliver useful information. The general tier or stack efficiency can be directly substituted by the regression relation ( 3 ), as well, as presented for the whole stack in Figure 9.

The losses between tier and stack layout are addressed in the current research by compressor and pump electric drive power inputs, subjected to assessment and optimization, as described below. Moreover, additional loss caused by variable water concentration at air side for a FC PEM with long way across a cell (visible clearly in the center of Figure 3) and power input of additional accessories, i.e.

$$\eta_{stack} = \frac{1}{1 + L_{rel,cell} (1 - L_{rel,tier}) (1 - L_{rel,stack}) + L_{rel,tier} (1 - L_{rel,stack}) + L_{rel,stack}}$$

$$L_{rel,stack} = \frac{L_{cell} \frac{L_{inh}}{L_{cell}}}{P_{net}} + L_{rel,K} + L_{rel,acc} =$$

$$= L_{rel,cell} (1 - L_{rel,tier}) (1 - L_{rel,stack}) \frac{\overline{\Delta C_{H2-H2O}}}{\Delta C_{H2-H2O,max}} + \frac{\sum_i P_{K,i}}{\eta_{eM} \eta_{e,mech} P_{net}} + \frac{\sum_i \Delta P_{K,i}}{\eta_{eM} \eta_{e,mech} P_{net}} + \frac{\sum_i P_{acc,i}}{P_{net}} \quad (7)$$

Inhomogeneity of concentration drop can be reflected by suitable mean effective concentration compared to maximum concentration difference at an elementary cell. The approach similar to temperature difference averaging in cross-flow heat exchangers can be used. The compressor power assessment is described below.

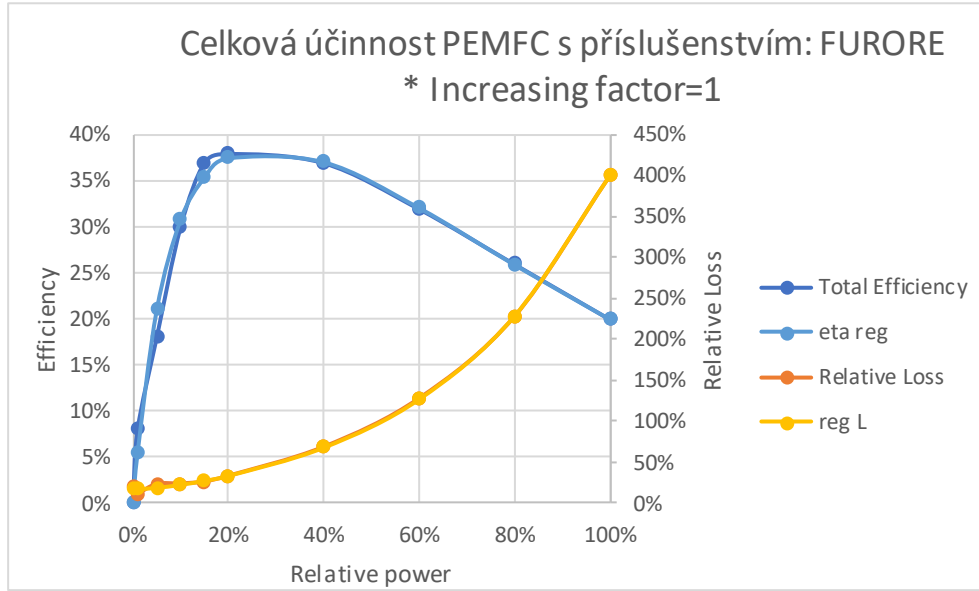


Figure 9 Regression model of stack efficiency from [1] based on model in [11]

### 3. Gas Properties for PEM FC Model

The temperatures of the whole PEM FC process are close to reference temperature for enthalpy computations, therefore the need for gas enthalpy simulation is not significant, seemingly. Nevertheless, the temperature derivative of specific enthalpy, specific isobaric thermal capacity should be calculated with higher accuracy due to the use of  $C_p/C_v - 1$  term in exponents for isentropic changes. Water steam is diluted and its partial pressures are low, but the temperature dependence of it should be respected for appropriate assessment of gas humidity and – if necessary – condensation to liquid water, especially in expansion turbine. That is why the standard regression formulas for enthalpy are used for all gases in consideration ( $O_2$ ,  $N_2$ ,  $H_2$ ,  $Ar$  and  $H_2O$ )

$$h_{gas} = (h_{ref,g-g}^{298.15} + \Delta H_0) + H_1 T + H_2 T^2 + H_3 T^3 + H_4 \sqrt{T} + H_5 \ln T$$

$$\frac{dh_{gas}}{dT} = c_p = H_1 + 2H_2 T + 3H_3 T^2 + \frac{H_4}{2\sqrt{T}} \sqrt{T} + \frac{H_5}{T} \quad (8)$$

Enthalpy of formation (gas-gas, equivalent to LCV) is based on steam and for water is negative, other elementary gases feature zero values. Regression constant  $\Delta H_0$  is close to zero. Specific enthalpy and specific gas constant of a mixture is calculated as scalar product of mass fractions and specific enthalpies, but it is more suitable to separate variable contents of steam and water using specific humidity as

$$h = \frac{h_{dry} + x_S h_{H_2O,S} + x_L h_{H_2O,L}}{1 + x_S + x_L} \quad (9)$$

Isobaric thermal capacity for  $T$  can be used for small temperature differences in compressors and turbines or mean values

$$c_{p,mean} = \frac{h_{in} - h_{out}}{T_{in} - T_{out}} \quad (10)$$

can be evaluated by iterations. If steam condenses to liquid water, the enthalpy is calculated by constant coefficient relation

$$h_{H_2O,L} = c_{p,H_2O} (T - T_{ref}) + h_{ref,H_2O,g-L}^{298.15} = c_{p,H_2O} (T - T_{ref}) + h_{ref,H_2O,g-g}^{298.15} - I_{H_2O} \quad (11)$$

The last term, containing latent heat of condensation, corrects reaction enthalpy to g-L conditions, i.e., to CV. All water and steam features are prepared for replacement by accurate IAPWS formulae [19]. However, it would extend the code significantly and cause long computation time with only very slight improvement of accuracy at pressures and temperatures currently occurring.

The iteration procedure for temperature evaluation from the enthalpy  $h$  is based on Newton-Raphson method as

$$T_{i+1} = T_i - \frac{H_0 + H_1 T_i + H_2 T_i^2 + H_3 T_i^3 + H_4 \sqrt{T_i} + H_5 \ln T_i - h}{H_1 + 2H_2 T_i + 3H_3 T_i^2 + \frac{H_4}{2\sqrt{T_i}} + \frac{H_5}{T_i}} \quad (12)$$

E.g., the employment of expansion turbine procedure requires solving outlet FC temperature from exhaust enthalpy, using (1) and then (12)

$$h_{FC,v,out} = \frac{\dot{m}_{air} h_{FC,air,in} + \dot{m}_{fuel} h_{FC,fuel,in} - (1 + K_{cool,P}) P_{gross} \eta_{net-gross}}{\dot{m}_{air} + \dot{m}_{fuel}} \quad (13)$$

The maximum cooling is limited by the condition of outlet temperature above the inlet one, i.e., limited by exhaust enthalpy at temperature of low-pressure compressor inlet under standard circumstances

$$K_{cool,P} \leq \frac{\dot{m}_{air} h_{FC,air,in} + \dot{m}_{fuel} h_{FC,fuel,in} - (\dot{m}_{air} + \dot{m}_{fuel}) h_{FC,v,out}}{P_{gross} \eta_{net-gross}} - 1 \quad (14)$$

The formulas for humidity of gases are based on standard relations for relative and specific humidity in dependence on gas pressure

$$x = \frac{\frac{r_{g,dry}}{r_{H2O}} \varphi p_{sat}}{p - \varphi p_{sat}} \quad (15)$$

Saturated steam pressure depends on temperature. Modified Rankine-Kirchhoff equation is used with regression coefficients from steam properties, e.g. from IAPWS [19]

$$p_{sat} = e^{A_0 + \frac{A_1}{T} + A_2 \ln T + A_3 T} \quad (16)$$

The accuracy for the temperatures in consideration is very good, see Figure 10.

If mass specific humidity is higher than its value for relative humidity of 100%, the excessive water mass is condensed and the enthalpy of relevant part of steam is substituted by liquid water enthalpy

$$x_{sat} = \frac{\frac{r_{g,dry}}{r_{H2O}} p_{sat}}{p - p_{sat}} \quad (17)$$

$$x_L = \max(0; x - x_{sat})$$

and

$$h = \frac{h_{g,dry} + x_S h_S + x_L h_L}{1 + x_S + x_L} \quad (18)$$

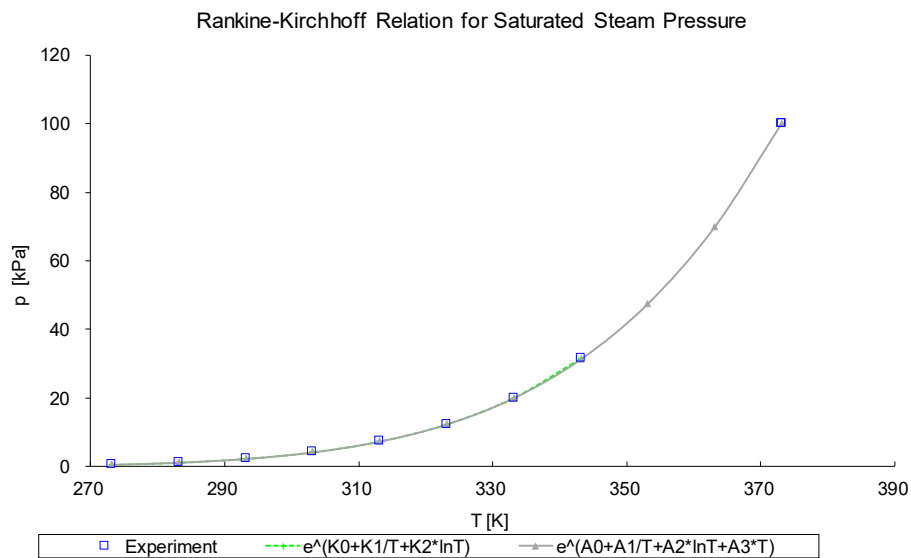


Figure 10 Regression model of saturated pressure/temperature dependence of steam, using modified Rankine-Kirchhoff relation

#### 4. Air Path Model

Compressors in air-path model – Figure 2 – are simulated by map-based approach. The procedures described in details in [20] or [21]. The basic relations are based on Eulerian theorem with regression of two parameters  $K$

$$\begin{aligned}
u_{K2} &= \frac{\pi D_{2K} n_K}{60}; \quad \rho_2 \approx \frac{p_{K1}}{2r_K T_{K1}} \left[ 1 + \frac{\pi_K T_{K1}}{T_{K2}} \right]; \quad w_{2r} = \frac{\dot{m}_K}{\pi D_{2K} b_{2K} \rho_2} \\
\Delta h_K &= K_1 u_{K2}^2 + K_2 w_{2r} u_{K2} = c_{pK} T_{K1} \frac{\pi_K^{\frac{\kappa-1}{\kappa}} - 1}{\eta_{KS}}; \quad T_{K2} = T_{K1} + \frac{\Delta h_K}{c_{pK}}
\end{aligned} \tag{19}$$

As understandable from ( 19 ), the value of isentropic efficiency is needed for enthalpy difference and outlet temperature relations.

Pressure ratio is either evaluated from pressures in compressor inlet and outlet (e.g., atmospheric pressure and boosted pressure at PEM FC inlet), or from compressor input power (see below). Regression coefficients from a transformed map (pressure ratio as a function of compressor speed and MFR) are presented in Figure 11. Compressor power, covered by electric input or by an expansion turbine, is

$$P_K = \Delta h_K \dot{m}_K = \dot{m}_K c_{pK} T_{K1} \frac{\pi_K^{\frac{\kappa-1}{\kappa}} - 1}{\eta_{KS}} \tag{20}$$

The pressure losses are taken into account in coupling relations, as, e.g.,

$$\pi_K = \frac{p_{next} + \Delta p_{K,out}}{p_{previous} - \Delta p_{K,in}} \tag{21}$$

Pressure losses are calculated for the averaged temperature and humidity. In the most general case of intercooler model, the outlet temperature is based on map cooling efficiency (and corrected to water condensation, if necessary). Pressure loss is composed of laminar friction term and inertia/turbulent term with powers of velocity of one or two, respectively. Due to low change of pressure, density is estimated from inlet pressure only, unlike temperature:

$$\begin{aligned}
T_{CH,out} &= T_{K2} + \eta_{CH} (T_{K2} - T_{CH,cool}) \\
\rho_{CH} &= \frac{p_{K2}}{r_K \left( T_{K2} + \frac{\eta_{CH}}{2} (T_{K2} - T_{CH,cool}) \right)}; \quad w_{CH} = \left( \frac{\dot{m}_K}{A_{CH} \rho_{CH}} \right) \\
p_{K2} &= p_{FC,inlet} + \Delta p_{CH}; \quad \Delta p_{CH} = \frac{\rho_{CH} w_{CH}^2}{2} \left( \frac{\zeta_{lam}}{w_{CH}} + \zeta_{CH} \right); \quad p_{K1} = p_a - \frac{\zeta_K}{2} \frac{\dot{m}_K^2 r_s T_a}{p_a A_{K1}^2}
\end{aligned} \tag{22}$$

Similar relation as for  $\Delta p_{CH}$  is used for a pressure drop across a PEM FC stack.



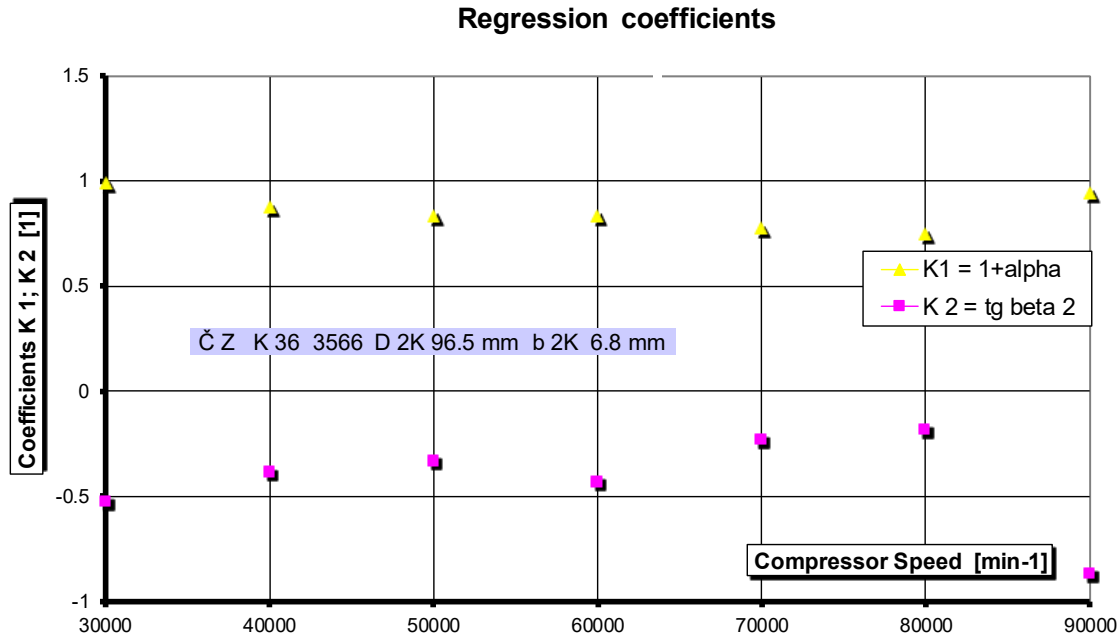


Figure 11 Regression coefficients for a model of compressor angular momentum equation

The compressor map is represented by regression in the form of polynomial fraction function, in which coefficients determined by linear regression method are functions of compressor speed, as plotted in Figure 12, are used in the following relation

$$\pi_K = \frac{p_{K2}}{p_{K1}} = \frac{a(n_{red}) \cdot \dot{m}_{red} + b}{-c(n_{red}) \cdot \dot{m}_{red}^2 - d(n_{red}) \cdot \dot{m}_{red} + 1} \quad (23)$$

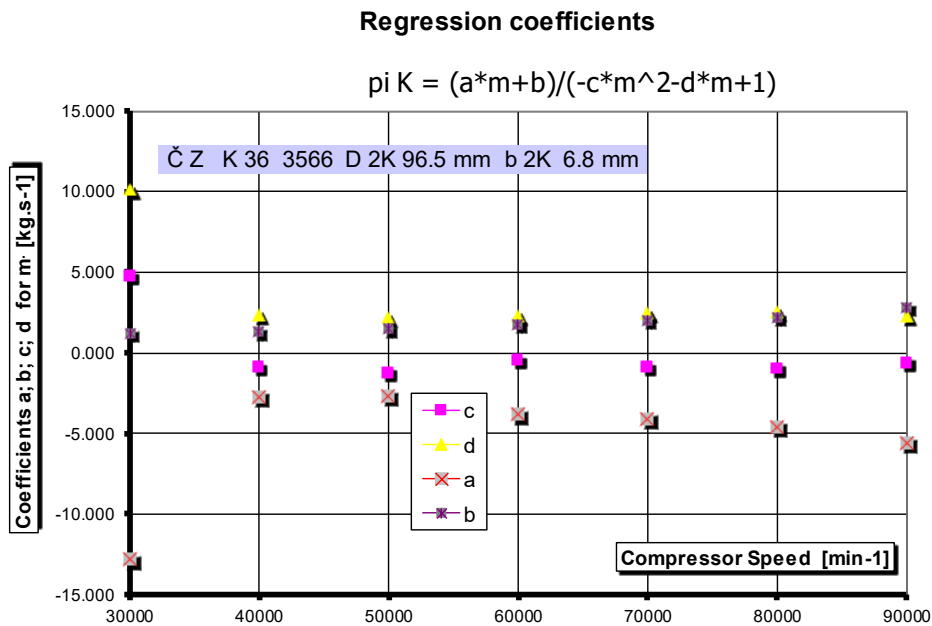


Figure 12 Regression coefficients for Eq. (23), characterizing a speed line in compressor map

Compressor map with extrapolation to very low pressure ratios is presented in Figure 13, efficiency curves are in Figure 14. The details on representation of surge limit and other compressor features are described in [21].

The maps for positive displacement compressors (e.g., EATON) can be used in the same manner except for reduction factor of MFR and speed, which does not use the square root of temperature for Mach number similarity. Only the changes of density at inlet need to be respected in appropriate reduction factor.

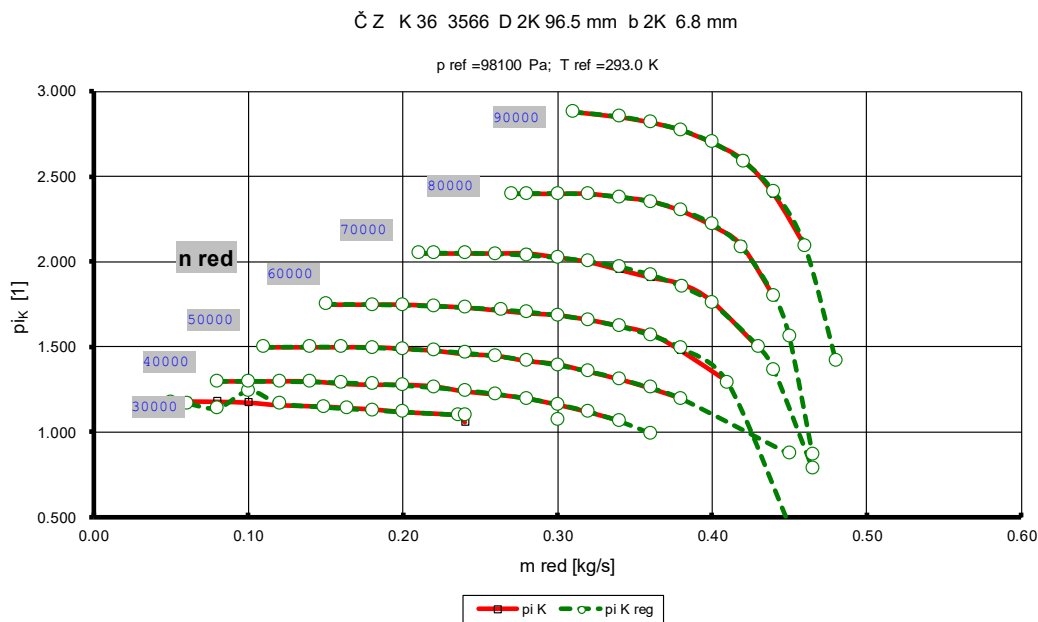


Figure 13 Compressor map pressure ratio speed-lines – comparison of measurement and regression substitution

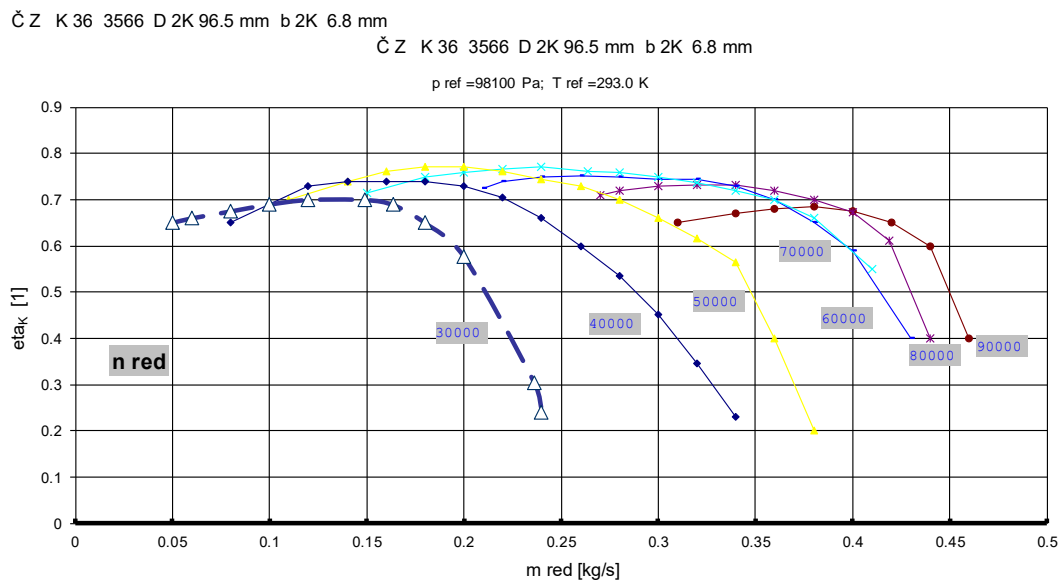


Figure 14 Compressor map efficiency speed lines

An expansion turbine MFR is described as the flow of compressible fluid through a single nozzle with correction discharge (turbine “swallowing”) coefficient and Saint-Venant-Wantzel flow function

$$\dot{m}_T = A_{T,ref} \mu_T \frac{p_{T1}}{\sqrt{r_v T_{T1}}} \sqrt{\Psi(p_{T2}/p_{T1})}; \quad \pi_T = p_{T1}/p_{T2} \quad (24)$$

Besides of  $\Psi$  function, discharge coefficient is significantly dependent on turbine pressure ratio, as well - Figure 15.

The power of a turbine is dependent on enthalpy difference, using standard relation between real and isentropic enthalpy drop reflected by turbine isentropic efficiency. Compressor power, if driven by an expansion turbine, takes turbine bearing friction losses into consideration.

$$P_T = \dot{m}_T \Delta h_T = \dot{m}_T c_{pT} T_{T1} \eta_{Ts} \left[ 1 - \left( \frac{p_{T2}}{p_{T1}} \right)^{\frac{\kappa_v - 1}{\kappa_v}} \right]; \quad p_{T1} = p_{FC,in} - \Delta p_{FC} \quad (25)$$

$$p_{T2} = p_a + \frac{\zeta_T}{2} \frac{\dot{m}_T^2 r_v T_{T2}}{\rho_a A_{T2}^2}; \quad T_{T2} = T_{T1} \left[ 1 - \eta_{Ts} \left[ 1 - \left( \frac{p_{T2}}{p_{T1}} \right)^{\frac{\kappa_v - 1}{\kappa_v}} \right] \right]$$

In the case of a turbocharger, compressor power equals to a turbine one, multiplied by a turbocharger mechanical efficiency. It makes determination of TC compressor pressure ratio possible. The rest to required boost pressure has to be covered by electrically driven compressor or by additional power supplied to a turbocharger shaft - Figure 19, in both cases using electric output from a PEM FC. This power has to be divided by electric motor efficiency including inverter losses and mechanical efficiency, as already presented in Eq. ( 7 ).

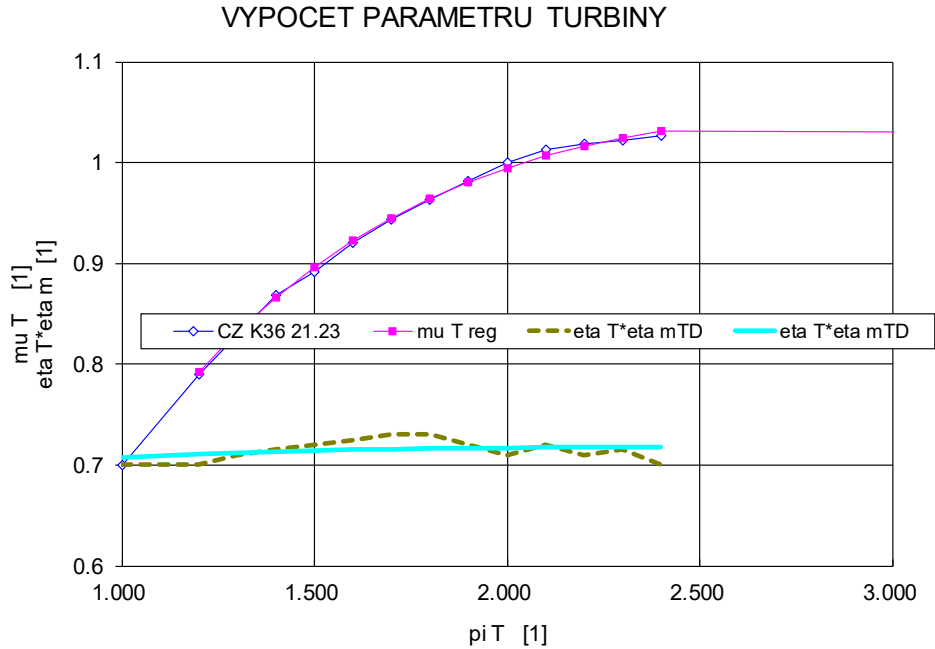


Figure 15 Regression model of turbine mass-flow rate discharge coefficient at the turbine speed in dependence on pressure ratio and turbine shaft efficiency including friction losses of bearings

## 5. The First Results

During de-bugging period, the code has been tested by sensitivity reactions. The result for air excess influence on FC power and efficiency is presented in Figure 16. The FC itself has not been simulated from the point of view of changed concentrations by charging.

Three case are compared: FC with combined TC and e-booster charging, FC without any boosting, but with coverage of FC proessure loss by electric charger and FC with fully electric drive of a compressor for boosting. Other factors (auxiliaries, etc.) were not simulated. The pressure loss parameters are kept at the same level (yet not calibrated).

The higher air excess is, the lower impact of compressor power to stack efficiency, especially if boosting is used. The positive effect of combined boosting with a TC is obvious but still the power intensification by boosting causes efficiency drop. Nevertheless, the pressure loss of unboosted FC causes also efficiency drop due to the driving power of a charger.

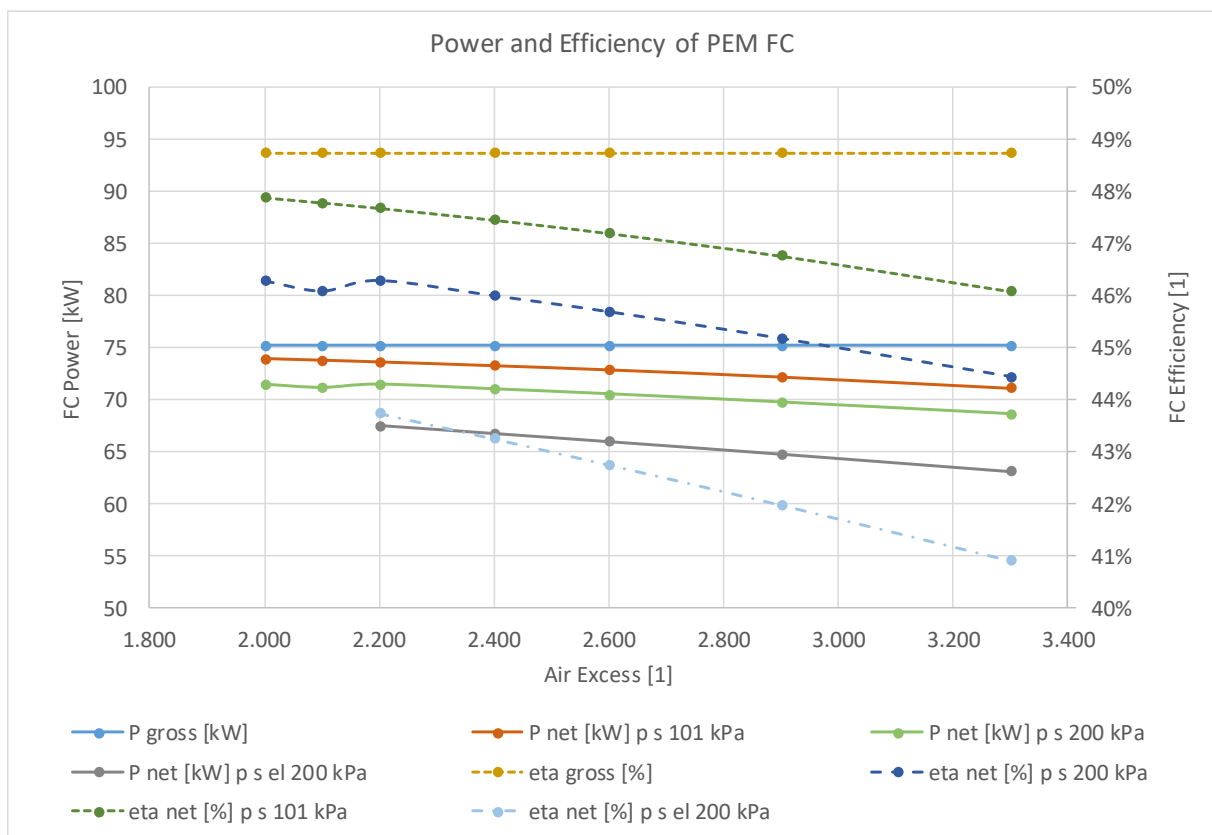


Figure 16 Impact of air excess on FC power and efficiency caused by compressor input power

The FC cooling was kept at level keeping outlet exhaust temperature, as presented in Figure 17 . In the case of expansion turbine use, the outlet temperature is significantly reduced unlike in other cases. The cold air causes water condensation but for the level of boosting limited by 200 kPa the outlet temperature yields no potential for FC cooling intensification. It would occur at higher pressure ratios. On the other hand, the danger of ice occurrence is also avoided, which is good for turbine reliability.

The relative cooling loss depends on the system of charging - Figure 18. The values are related – for comparison – to both fixed gross power and variable net power. The lowest demands are in the case of unboosted system with the highest efficiency. The apparently high cooling power in the case of a

TC in comparison to electrical boosting is caused by the overall small net power of the latter case. The additional demands on intercooling are not involved in Figure 18.

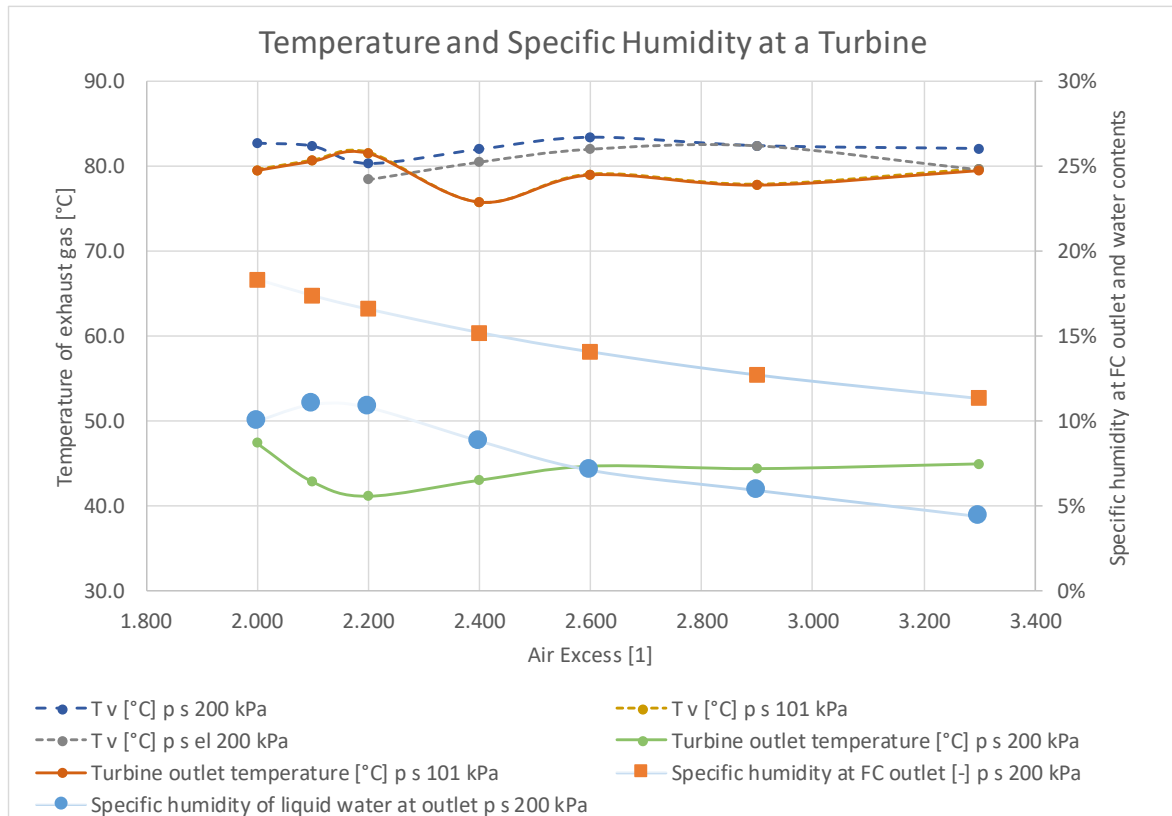


Figure 17 Impact of air excess on FC temperatures and exhaust humidity

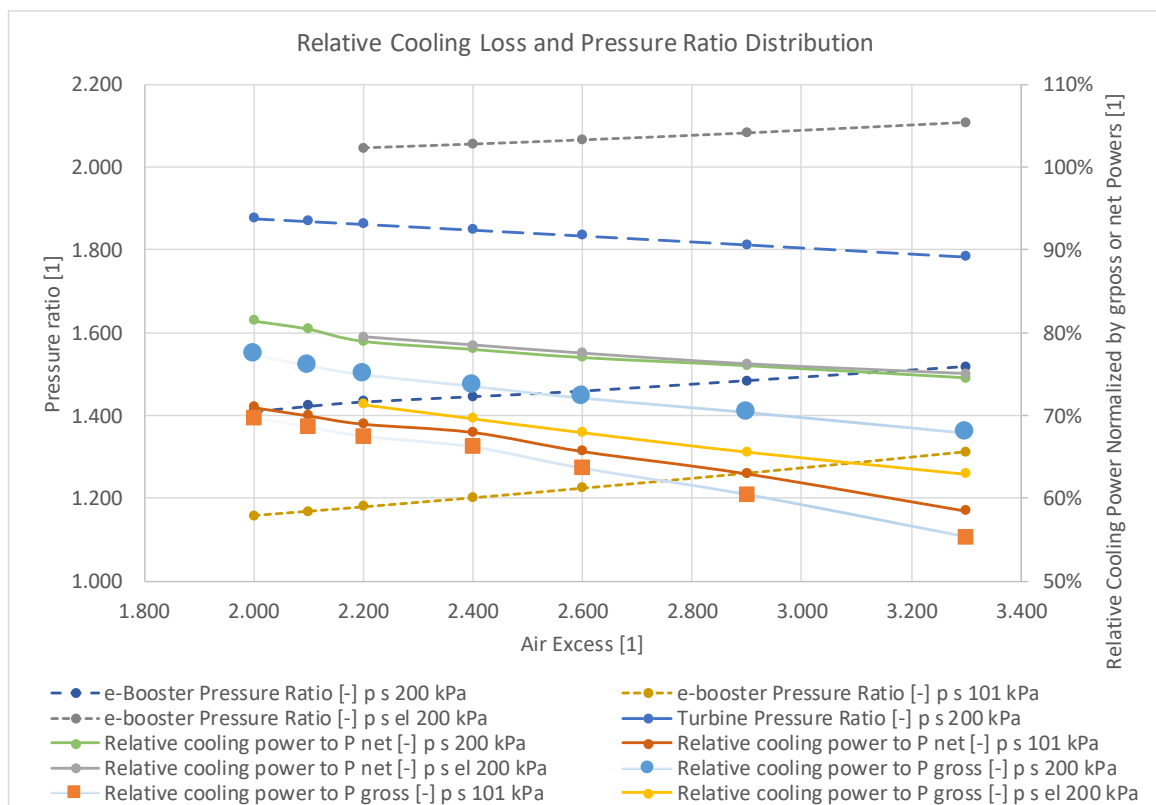


Figure 18 Impact of air excess on charging group pressure ratios and relative cooling loss



## 6. Possibilities of Compressor and Turbocharger Procurement

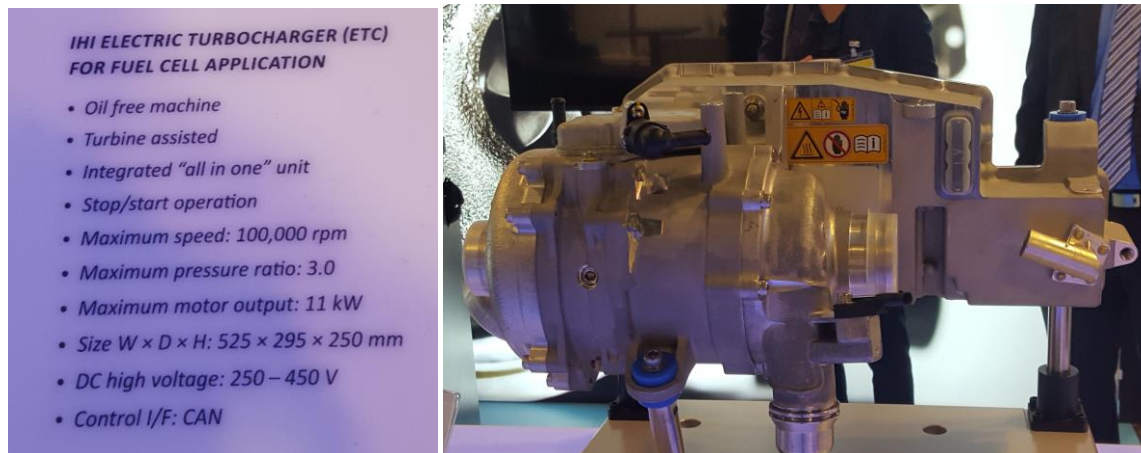


Figure 19 IHI e-turbocharger for PEM FC driven Mercedes Benz class GLC of estimated. 150 – 200 kW FC power- Aachener Kolloquium 2019, Jan Macek- [5]

All gas treating machines have to exclude any lubricating oil contamination. That is why oil-free active parts have to be used. The solution is in using gas bearings (e.g. ATEKO [7]). Other possible contacts with pre-negotiated possibility of receiving offers for parameters investigated during project elaboration, are at Garrett Motion [4], IHI European subsidiary [5] or at Eaton [6].

## 7. Conclusion

The goals set for the first period of project activities have been fulfilled.

The simulation code reflects power consumption by boosting and side effects, as water condensation. The data obtained from it will be compared to commercial code results after the calibration of prepared modules. The form of the model is suitable for the following optimization.

The first results show the way for improving the stack parameters.

Contacts for compressor procurements for a full scale FCs in the future were established during the first year of project elaboration.

The future work is fully covered by planned calibration and optimization period inside WP 2C during the year 2020.

The impact of air pressure and air excess on cell efficiency is on one hand out of the scope of the C-part of the project, but it may be involved into the simulation yielding more complex picture of the air path design results. The possibilities of using expanded cold humid air for FC cooling intensification will be taken into account, as well.

The results of 2019 year experiments will be included into the simulation codes and extrapolated by them into full-scale proposals.

## 8. Symbols and Acronyms

$A$	area of cross-section [m <sup>2</sup> ]
$A, a, \dots, e$	regression parameters
$b$	width [m]
$C$	concentration [kmol.m <sup>3</sup> ]
$c$	specific thermal capacity [J.kg <sup>-1</sup> .K <sup>-1</sup> ]
$D$	diameter [m]
$H_u$	LCV of reference fuel [J.kg <sup>-1</sup> ]
$h$	specific enthalpy [J.kg <sup>-1</sup> ]
$I$	electric current [A]
$K$	general regression constant
$L$	time-rate of losses [W]
$L_t$	stoichiometric (humid)air-to-(humid)fuel ratio [1]
$l_{H_2O}$	specific latent heat of condensation at very low partial pressure [J.kg <sup>-1</sup> ]
$\dot{m}$	MFR [kg.s <sup>-1</sup> ]
$n$	speed [min <sup>-1</sup> ]
$P$	power [W]
$p$	pressure [Pa]
$R$	electric resistance [Ω]
$r$	specific gas constant [J.kg <sup>-1</sup> .K <sup>-1</sup> ]
$T$	temperature [K]
$U$	electric voltage [V]
$u$	blade speed [m.s <sup>-1</sup> ]
$w$	flow relative velocity [m.s <sup>-1</sup> ]
$x$	specific humidity [kg H <sub>2</sub> O/kg dry gas]
$\Delta$	difference or correction
$\eta$	efficiency [1]
$\zeta$	pressure loss coefficient [1]
$\kappa$	$c_p/c_v$ [1]
$\lambda$	air excess, relative air-to-fuel ratio [1]
$\mu$	discharge coefficient [1]
$\pi$	pressure ratio, Ludolf number [1]
$\rho$	density [kg.m <sup>-3</sup> ]
$\sigma$	mass fraction [1]
$\varphi$	relative humidity [1]
$\Psi$	MFR-pressure function [1]

## Subscripts

<i>a</i>	atmospheric
<i>acc</i>	accessory
<i>air</i>	air
<i>cell</i>	elementary FC cell with constant concentration in a cross-flow of both reactants
<i>CH</i>	intercooler
<i>cool</i>	cooling liquid or ... to cooling liquid
<i>dry</i>	dry gas mixture
<i>eM</i>	electric motor
<i>FC</i>	fuel cell
<i>fuel</i>	fuel, humid hydrogen
<i>g</i>	gaseous phase
<i>gross</i>	gross (tier) internal power of a FC
<i>i</i>	iteration or summation subscript
<i>in</i>	inlet
<i>inh</i>	concentration and/or temperature inhomogeneity
<i>K</i>	compressor
<i>L</i>	liquid
<i>lam</i>	at laminar flow
<i>mech</i>	mechanical (friction) losses
<i>net</i>	net (external, "brake") FC power
<i>out</i>	outlet
<i>p</i>	constant pressure
<i>r</i>	radial direction
<i>red</i>	reduced or corrected MFR for turbomachinery
<i>ref</i>	reference state at 298.15K with zero enthalpy of formation for chemical elements
<i>rel</i>	relative, normalized by power in the case of losses or by rated power in the case of
power	
<i>S</i>	steam
<i>s</i>	constant entropy; FC inlet
<i>sat</i>	saturated
<i>stack</i>	FC stack
<i>tier</i>	FC tier
<i>T</i>	Turbine

$v$	exhaust; constant volume
1	inlet, upstream
2	outlet, downstream

### Acronyms

BSR	blade-speed ratio for turbines
CV	calorific value
FC	fuel cell
LCV	lower calorific value
MFR	mass-flow rate
PEM	proton or polymer exchange membrane
TC	turbocharger

## 9. References

- [1] Affenzeller, J., Internal materials from Technological Platform Project EU FP5 FUIRORE, 2005, Prague 2007
- [2] Internal Sources from EU FP6 Project Roads to Hydrogen Communities [www.roads2hy.com](http://www.roads2hy.com) 2008, nyní [https://cordis.europa.eu/publication/rcn/11063\\_en.html](https://cordis.europa.eu/publication/rcn/11063_en.html)
- [3] Manual and On-line Help for GT Suite Code, Beta version 2019, Gamma Technologies 2019, [www.gtisoft.com](http://www.gtisoft.com)
- [4] [petr.skara@garrettmotion.com](mailto:petr.skara@garrettmotion.com)
- [5] [i.durbiano@ihi-csi.de](mailto:i.durbiano@ihi-csi.de)
- [6] [LudekJanik@eaton.com](mailto:LudekJanik@eaton.com)
- [7] Pavel Schustr [pavel.schustr@email.cz](mailto:pavel.schustr@email.cz)
- [8] Adam Z. Weber and John Newman, Modeling Transport in Polymer-Electrolyte Fuel Cells. Chem. Rev. 2004, 104, 4679-4726
- [9] A. A. Kulikovskiy, Quasi-3D Modeling of Water Transport in Polymer Electrolyte Fuel Cells. Journal of The Electrochemical Society, 150 (11) A1432-A1439, 2003. DOI: [10.1149/1.1611489]
- [10] Benedikt Hollweck, Thomas Korb, Gregor Kolls, Timo Neuner, Jörg Wind, Analyses of the holistic energy balance of different fuel cell powertrains under realistic boundary conditions and user behaviours. WHTC Congress Prague 2017, prepare for publication in Journal of Hydrogen Technology, Elsevier
- [11] Macek, J., Morkus, J., Kolář, J., Model Of Surface Vehicle Fleet Energy Consumption Suitable For Climate-Energy Policy Assessment. L. Conference Of Czech And Slovak University Departments And Institutions Dealing With The Research Of Internal Combustion Engines, Mendel University In Brno, Faculty Of Agrisciences, 2019. pp. 110-123
- [12] Macek, J., Problémy modelování oběhů používajících vodu, vodní páru a jejich směsi s plyny v pístových motorech. XXXVI. mezinárodní konference kateder a pracovišť spalovacích motorů českých a slovenských vysokých škol, 2005
- [13] MACEK, J., MORKUS, J., "Optimum Limits of Motor Vehicle Driving", XLVIIIth Conference Of Czech And Slovak Combustion Engine Research, Technical University of Liberec, 2017
- [14] MACEK, J., MORKUS, J., DENK, P., STEINBAUER, P., VÍTEK, O., TOMAN, R., Optimization Tool for Hybrid Vehicles, XLIX. International scientific conference of the Czech and Slovak Universities' Departments and Institutions Dealing with the Research of Combustion Engines, „KOKA 2018“, Nitrianske Rudno 19-21. 9. 2018, SLOVAK REPUBLIC
- [15] MACEK, J., STEINBAUER, P., MORKUS, J., ŠIKA, Z., Optimization of Road Energy Consumption in Hybrid Vehicles. SAE/ATA Conference on Reduction of CO2 Emissions, Torino 2018.
- [16] STEINBAUER, P.; MACEK, J.; MORKUS, J.; DENK, P.; ŠIKA, Z.; PASTEUR, F., Aspects for Velocity Profile Optimization for Fleet Operated Vehicles. In: Comprehensive Energy Management – Eco Routing & Velocity Profiles. Basel: Springer, 2017. p. 1-18. ISBN 978-3-319-53165-6.
- [17] STEINBAUER, P.; HUSÁK, J.; DENK, P.; MACEK, J.; ŠIKA, Z.; PASTEUR, F., Predictive control of commercial e-vehicle using a priori route information. International Journal of Powertrains. 2018, 2018(7), 53-71. ISSN 1742-4275.
- [18] STEINBAUER, P.; MACEK, J.; MORKUS, J.; DENK, P.; ŠIKA, Z.; BARÁK, A., Dynamic Optimization of the E-Vehicle Route Profile, In: SAE Technical Paper 2016-01-0156. Warrendale, PA: SAE International, 2016.
- [19] IAPWS: Release on the IAPWS Formulation 1997 for the Thermodynamic Properties of Water and Steam for Industrial Use. The International Association of for the Properties of Water and Steam, Erlangen 1997, 48 s.



- [20] Macek, J. - Polášek, M. - Šika, Z. - Florián, M.: Simplification of Transient Response Models for ICE Management In: MECCA Journal of Middle European Construction and Design of Cars. 2005, vol. 3, no. 2+3, s. 32-41. ISSN 1214-0821.
- [21] Jan Macek, Miloš Polášek, Zbyne k Šika, Michael Valášek, Martin Florián, Oldrich Vitek, Transient Engine Model as a Tool for Predictive Control. SAE Paper 2006-01-0659, SAE Warrendale 2006

Relative humidity  $x_v$  is fixed. For the case of relative humidity over 100%, one part of water steam condenses to  $x_{vL}$  and the rest  $x_{vS}$  is in the state of saturated steam.

### Start of iteration

$$g = O_2; N_2; Ar; H_2; H_2O, S$$

$$h_g = (h_{ref,g-g}^{298.15} + \Delta H_{0,g}) + H_{1,g}T + H_{2,g}T^2 + H_{3,g}T^3 + H_{4,g}\sqrt{T} + H_{5,g}\ln T$$

$$\frac{dh_g}{dT} = c_{p,g} = H_{1,g} + 2H_{2,g}T + 3H_{3,g}T^2 + \frac{H_{4,g}}{2\sqrt{T}}\sqrt{T} + \frac{H_{5,g}}{T}$$

$$h_{dry} = \sum_{g=O_2, N_2, Ar, H_2} h_g \sigma_{dry,g}$$

$$\frac{dh_{dry}}{dT} = \sum_{g=O_2, N_2, Ar, H_2} \sigma_{dry,g} \frac{dh_g}{dT}$$

$$h_{H_2O,L} = c_{p,H_2O}(T - T_{ref}) + h_{ref,H_2O,g-L}^{298.15} = c_{p,H_2O}(T - T_{ref}) + h_{ref,H_2O,g-g}^{298.15} - l_{H_2O}$$

$$\frac{dh_{H_2O,L}}{dT} = c_{p,H_2O}$$

$$p_{sat,v,i} = e^{A_0 + \frac{A_1}{T_{v,i}} + A_2 \ln T_{v,i} + A_3 T_{v,i}}$$

$$\frac{dp_{sat,v,i}}{dT} = \left( A_3 - \frac{A_1}{T_{v,i}^2} + \frac{A_2}{T_{v,i}} \right) p_{sat,v,i}$$

$$x_{sat,v,i} = \frac{\frac{r_{g,dry}}{r_{H_2O}} p_{sat,v,i}}{p_v - p_{sat,v,i}}$$

$$\text{If } p_{sat,v,\lim} = \frac{x_v p_v}{\frac{r_{g,dry}}{r_{H_2O}} + x_v} \stackrel{?}{<} p_{sat,v,i} = e^{A_0 + \frac{A_1}{T_{v,i}} + A_2 \ln T_{v,i} + A_3 T_{v,i}}$$

no condensation, i.e.,

$$x_{v,S,i} = x_v$$

$$x_{v,L,i} = 0$$

$$h_{v,i} = \frac{h_{dry,v,i} + x_v h_{H_2O,S,v,i}}{1 + x_v}$$

$$\frac{\partial x_{v,S,i}}{\partial T} = 0$$

$$\frac{\partial h_{v,i}}{\partial T} = \frac{1}{1 + x_v} \left( \frac{dh_{dry,v,i}}{dT} + x_{v,S,i} \frac{dh_{H_2O,S,v,i}}{dT} \right) = c_p \Big|_T$$

else

$$x_{v,S,i} = x_{sat,v,i}$$

$$x_{v,L,i} = x_v - x_{sat,v,i}$$

$$h_{v,i} = \frac{h_{dry,v,i} + x_{v,S,i} h_{H2O,S,v,i} + x_{v,L,i} h_{H2O,L,v,i}}{1 + x_v} = \frac{h_{dry,v,i} + x_{v,S,i} (h_{H2O,S,v,i} - h_{H2O,L,v,i}) + x_v h_{H2O,L,v,i}}{1 + x_v}$$

$$\frac{\partial x_{v,S,i}}{\partial T} = \frac{r_{g,dry}}{r_{H2O}} \frac{\frac{dp_{sat,v,i}}{dT} (p_v - p_{sat,v,i}) + \frac{dp_{sat,v,i}}{dT} p_{sat,v,i}}{(p_v - p_{sat,v,i})^2}$$

$$\frac{\partial h_{v,i}}{\partial T} = \frac{1}{1 + x_v} \left( \frac{dh_{dry,v,i}}{dT} + \frac{dx_{v,S,i}}{dT} (h_{H2O,S,v,i} - h_{H2O,L,v,i}) + x_{v,S,i} \left( \frac{dh_{H2O,S,v,i}}{dT} - c_{p,H2O} \right) + x_v c_{p,H2O} \right) = c_p \Big|_T$$

$$\frac{\partial x_{v,S,i}}{\partial p} = - \frac{r_{g,dry}}{r_{H2O}} \frac{p_{sat,v,i}}{(p_v - p_{sat,v,i})^2}$$

$$\frac{\partial h_{v,i}}{\partial p} = \frac{\frac{\partial x_{v,S,i}}{\partial p} (h_{H2O,S,v,i} - h_{H2O,L,v,i})}{1 + x_v}$$

end if

$$c_p \Big|_{T_{in}}^{T_{out}} \approx \frac{c_p \Big|_{T_{in}}^{T_{out}} + c_p \Big|_{T_{in}}^{T_{in}}}{2}$$

$$r \Big|_T \approx \frac{\sum_d \sigma_{g,d} r_d + x_s r_{H2O} + x_L * 0}{1 + x_s + x_L}$$

$$r \Big|_{T_{in}}^{T_{out}} \approx \frac{r \Big|_{T_{in}}^{T_{out}} + r \Big|_{T_{in}}^{T_{in}}}{2}$$

$$\kappa = \frac{c_p \Big|_{T_{in}}^{T_{out}}}{c_p \Big|_{T_{in}}^{T_{out}} - r \Big|_{T_{in}}^{T_{out}}}$$

$$\Delta h_T = c_p \Big|_{T_{in}}^{T_{out}} T_{in} \left( 1 - \frac{1}{\pi^{\frac{\kappa_T - 1}{\kappa_T}}} \right) \eta_{T,s}$$

$$\Delta h_K = c_p \Big|_{T_{in}}^{T_{out}} T_{in} \frac{\left( \frac{\pi^{\frac{\kappa_K - 1}{\kappa_K}} - 1 \right)}{\eta_{K,s}}$$

$$h_{out,T} = h_{in} - \Delta h_T$$

$$h_{out,K} = h_{in} + \Delta h_K$$

and iteration for **T** from **Start**

$$h = \frac{h_{dry} + x_s (h_{H2O,S} - h_{H2O,L}) + x h_{H2O,L}}{1 + x}$$

$$\frac{\partial x_s}{\partial T} = \frac{r_{g,dry}}{r_{H2O}} \frac{\frac{dp_{sat}}{dT} (p - p_{sat}) + \frac{dp_{sat}}{dT} p_{sat}}{(p - p_{sat})^2}$$

$$\frac{\partial h}{\partial T} = \frac{1}{1 + x} \left( \frac{\partial h_{dry}}{\partial T} + \frac{\partial x_s}{\partial T} (h_{H2O,S} - h_{H2O,L}) + x_s \left( \frac{\partial h_{H2O,S}}{\partial T} - c_{p,LH2O} \right) + x c_{p,LH2O} \right) = c_p \Big|_T$$

$$\frac{\partial x_s}{\partial p} = - \frac{r_{g,dry}}{r_{H2O}} \frac{p_{sat}}{(p - p_{sat})^2}$$

$$\frac{\partial h}{\partial p} = \frac{\frac{\partial x_s}{\partial p} (h_{H2O,S} - h_{H2O,L})}{1 + x}$$

$$dq = dh - vdp = 0$$

$$0 = \frac{\partial h}{\partial T} dT + \left( \frac{\partial h}{\partial p} - \frac{1}{\rho} \right) dp$$

$$0 = c_p \Big|_T \frac{dT}{T} + \left( - \frac{r_{g,dry}}{r_{H2O}} \frac{p_{sat} \rho}{(p - p_{sat})^2} \frac{(h_{H2O,S} - h_{H2O,L})}{1 + x} - 1 \right) \frac{dp}{\rho}$$

If  $\kappa$  is too close to 1 then

$$\Delta h_T = r_{in}^{out} T_{in} \ln \frac{p_{in}}{p_{out}} \eta_{T,s}$$

$$\Delta h_K = \frac{r_{in}^{out} T_{in} \ln \frac{p_{out}}{p_{in}}}{\eta_{K,s}}$$

$$h_{out,T} = h_{in} - \Delta h_T$$

$$h_{out,K} = h_{in} + \Delta h_K$$